Rapid Communications

Sample dependence of half-integer quantized thermal Hall effect in the Kitaev spin-liquid candidate α-$RuCl_3$

M. Yamashita,[1,*] J. Gouchi,[1] Y. Uwatoko,[1] N. Kurita,[2] and H. Tanaka[2]
[1]*Institute for Solid State Physics, The University of Tokyo, Kashiwa, 277-8581, Japan*
[2]*Department of Physics, Tokyo Institute of Technology, Tokyo 152-8551, Japan*

(Received 27 April 2020; revised 13 November 2020; accepted 23 November 2020; published 7 December 2020)

We have investigated the sample dependence of the half-integer thermal Hall effect in α-$RuCl_3$ under a magnetic field tilted 45° from the c axis to the a axis. We find that the sample with the largest longitudinal thermal conductivity κ_{xx} shows the half-integer quantized thermal Hall effect expected in the Kitaev model. On the other hand, the quantized thermal Hall effect was not observed in the samples with smaller κ_{xx}. We suggest that suppressing the magnetic scattering effects on the phonon thermal conduction, which broaden the field-induced gap protecting the chiral edge current of the Majorana fermions, is important to observe the quantized thermal Hall effect.

DOI: 10.1103/PhysRevB.102.220404

Nontrivial topology in a condensed-matter state realizes a quantization of a physical quantity. One of the most fundamental examples is the quantized Hall conductivity in a quantum Hall system, where the quantized Hall conductivity is given by the Chern number determined by the topology of the system [1].

A new intriguing case of this topological quantization is a Kitaev magnet [2,3]. In the Kitaev model, localized spin-1/2 moments on a two-dimensional (2D) honeycomb structure are coupled to each other by bond-dependent Ising interactions. The frustration effect of this Kitaev Hamiltonian prevents the spins from ordering even at zero temperature, realizing a quantum spin-liquid (QSL) state. Remarkably, this ground state of the Kitaev Hamiltonian is exactly solvable. The ground state has been shown to be characterized by two kinds of elementary excitations: itinerant Majorana fermions and localized Z_2 fluxes. In a magnetic field, these itinerant Majorana fermions have topologically nontrivial gapped bands with Chern number $C = \pm 1$, giving rise to a quantized chiral edge current. In contrast to a quantized chiral edge current of electrons in a quantum Hall system, this chiral edge current is carried by the charge-neutral Majorana fermions. Therefore, this quantized chiral edge current has been predicted to appear in the 2D thermal Hall conductivity as $\kappa_{xy}^{2D}/T = (C/2)q_t$, where $q_t = (\pi/6)k_B^2/\hbar$.

Materializing the Kitaev model has been suggested in several Mott insulators with strong spin-orbit coupling [4]. One of the most studied Kitaev candidates is α-$RuCl_3$, in which a 2D honeycomb structure of edge-sharing $RuCl_6$ octahedra was shown to have a dominant Kitaev interaction [5–7]. Various measurements [8–13] reported Kitaev-like signatures above the antiferromagnetic (AFM) ordering temperature of $T_N \sim 7$ K (Refs. [8,14–16]). This magnetic order can be suppressed by applying a magnetic field of ∼8 T in the a-b plane [14,17,18], enabling one to study the Kitaev QSL down to lower temperatures. Most remarkably, thermal Hall measurements done under an in-plane field have shown the half-integer quantized thermal Hall conduction [19,20], indicating the presence of a chiral edge current of the Majorana fermions protected by the field-induced gap. However, details of this field-induced gap are unknown because the Kitaev Hamiltonian loses its exact solvability in a magnetic field.

It has been reported that this quantized thermal Hall effect has a sample dependence associated with the longitudinal thermal conductivity κ_{xx} [20]. This κ_{xx} dependence may imply a scattering effect on the field-induced gap protecting the chiral edge current. A similar scattering effect was discussed in the intrinsic anomalous Hall effect (AHE) in ferromagnetic metals [21], where a broadening of the gap by scattering effects is suggested to destroy the intrinsic AHE in a less conductive metal. Therefore, further studies of the κ_{xx} dependence of this quantized thermal Hall effect may provide information about the unknown field-induced gap. It is also important to confirm the reproducibility of the quantized thermal Hall effect.

In this Rapid Communication, we report the sample dependence of the longitudinal (κ_{xx}) and transverse (κ_{xy}) thermal conductivity of three single crystals of α-$RuCl_3$. We confirm the reproducibility of the half-integer quantized thermal Hall effect in the sample showing the largest κ_{xx} among the three crystals. On the other hand, the other samples with smaller κ_{xx} show κ_{xy} much smaller than the value expected for the quantization. We also find that a sample with a larger κ_{xx} shows a larger decrease of the magnetic susceptibility below T_N, in addition to a larger field-increase effect of κ_{xx}, showing that magnetic scattering effects are more strongly suppressed by magnetic fields in a sample with better quality. From these results, we suggest that suppressing this magnetic scattering effect plays an important role in realizing the quantized thermal Hall effect.

*my@issp.u-tokyo.ac.jp

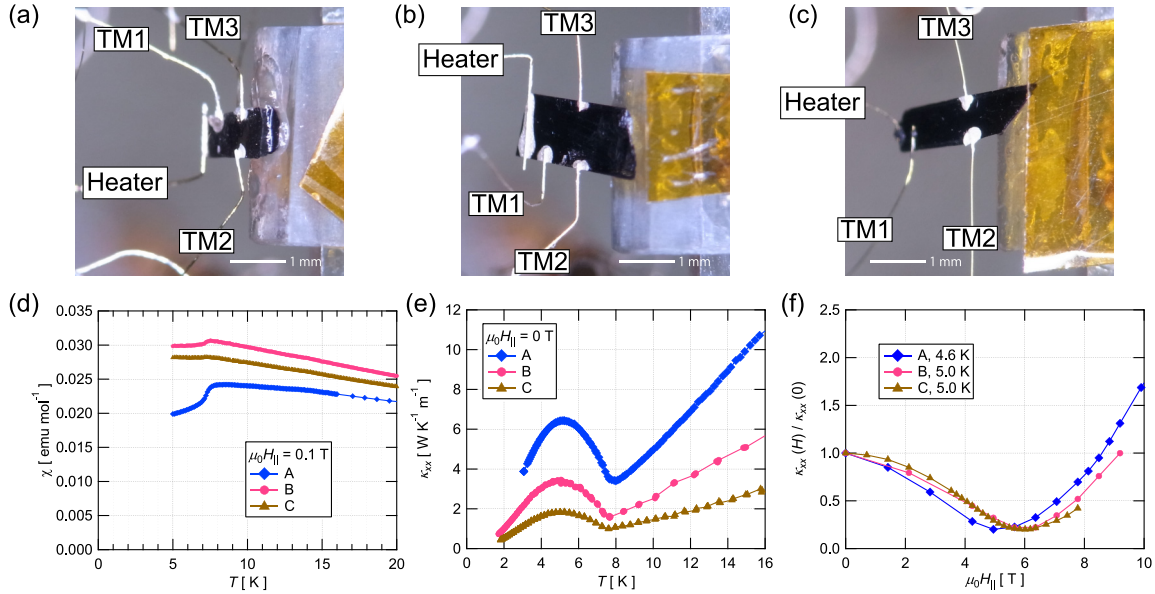

FIG. 1. (a)–(c) Setup pictures of the thermal conductivity and the thermal Hall measurements of samples A, B, and C, respectively. Note that these pictures were taken at different angles to the crystal. The thermal connections to the heater and the three thermometers (TM1–TM3) are indicated in each picture. The heat current was applied along the a axis (the long axis of the crystal), and the magnetic field was applied 45° from the c axis to the a axis. (d) The temperature dependence of the magnetic susceptibility at 0.1 T applied along the a axis. (e) The temperature dependence of the longitudinal thermal conductivity κ_{xx} at zero field. (f) The field dependence of κ_{xx} at 4.6 K (sample A) and at 5.0 K (samples B and C). The vertical axis is normalized by the zero-field value $\kappa_{xx}(0)$. The horizontal axis shows the in-plane field $\mu_0 H_{\parallel} = \mu_0 H/\sqrt{2}$.

Single crystals used in this work were synthesized by the Bridgman method as described in Ref. [14]. We have measured both κ_{xx} and κ_{xy} of three single crystals (samples A–C) of α-$RuCl_3$. A typical sample size was $2.5 \times 1.0 \times 0.03$ mm^3. These thermal-transport measurements were done by using a one-heater, three-thermometer method [see Figs. 1(a)–1(c)] as described in Ref. [22]. The measurement cell was the same as that used for a previous work (sample 2 in Ref. [13]). A heat current was applied along the a axis of the sample, and a magnetic field H was applied 45° from the c axis to the a axis. We denote the in-plane field $\mu_0 H_{\parallel}$ as $\mu_0 H_{\parallel} = \mu_0 H/\sqrt{2}$. We note that, because α-$RuCl_3$ is easily deformed owing to the van der Waals structure, it is important to carefully handle α-$RuCl_3$ to avoid applying stresses to the sample. However, some degree of stress is unavoidable, especially when taking a single crystal out of the chunk of crystals obtained by the Bridgman method. Therefore, we checked the sample quality by the magnetic susceptibility and κ_{xx} measurements prior to κ_{xy} measurements.

The temperature dependence of the magnetic susceptibility χ was checked for all samples prior to the thermal conductivity measurements [Fig. 1(d)]. To avoid the effect of the in-plane anisotropy of χ [23], the magnetic field was applied along the a axis for all the χ measurements. As shown in Fig. 1(d), no anomaly is observed at 14 K, showing an absence of the additional magnetic transition caused by stacking faults [14,16]. We further checked the sample quality by heat capacity measurements performed after the thermal-transport measurements. We confirmed that the anomaly from the additional magnetic transition is absent or small in all samples [24]. The AFM transition at $T_N \sim 8$ K is clearly seen in all samples. The largest decrease of $\chi(T)$ below T_N is observed in sample A. This decrease is smaller in sample B and the smallest in sample C.

Figure 1(e) shows the temperature dependence of κ_{xx} at zero field. As shown in Fig. 1(e), κ_{xx} of all samples shows a temperature dependence very similar to that of previous works [13,19,20,25,26]. The magnetic transition to the AFM phase is clearly seen by the onset of the increase of κ_{xx} below T_N. On the other hand, the magnitude of κ_{xx} is very different for each sample; κ_{xx} of sample A is the largest among the samples and is 4 times larger than that of sample C. A difference in the magnitude of κ_{xx} in the same compounds is given by the difference in the mean free path of the heat carriers [27], which reflects the scattering strength of the carriers. Therefore, this large sample dependence in the magnitude of κ_{xx}, compared to that in χ, shows a high sensitivity of κ_{xx} measurements to the sample quality. Also, this sample dependence of κ_{xx} correlates well to that of the decrease of χ below T_N. A sample with a larger decrease of χ below T_N shows a larger κ_{xx}.

Figure 1(f) shows the field dependence of κ_{xx} at ~5 K. By normalizing the zero-field value of each sample, a very similar field dependence can clearly be seen. As shown in Fig. 1(f), $\kappa_{xx}(H)/\kappa_{xx}(0)$ of all samples shows the minimum of κ_{xx} at an in-plane field of $H_{min} = 5$–6 T, which corresponds to the critical field of the AFM phase [14,17,18]. Above the critical field, $\kappa_{xx}(H)$ increases with increasing field. This increase is larger in a sample with a larger κ_{xx}.

The field dependence of the thermal Hall conductivity at different temperatures is shown in Fig. 2. For comparison, the value corresponding to the half-integer quantized thermal Hall $\kappa_{xy}^{2D}/(Td) = \pm q_t/(2d)$, where $d = 0.57$ nm is the distance between the 2D honeycomb layers of $RuCl_3$, is shown by the dashed lines.

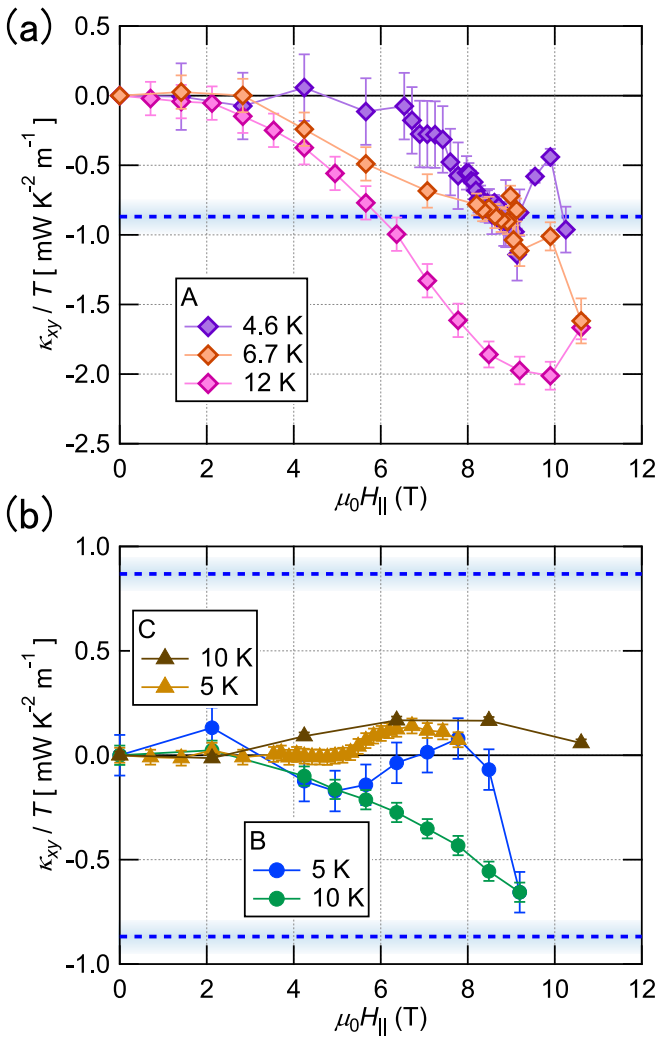

FIG. 2. The field dependence of the thermal Hall conductivity divided by the temperature κ_{xy}/T of (a) sample A and (b) samples B and C. The dotted lines show the value corresponding to the half-integer quantized thermal Hall effect (see the text for details).

As shown in Fig. 2, the sign of κ_{xy}/T at 10 K is negative in sample A and sample B, whereas it is positive in sample C. This sample dependence may be related to the angle between the a axis and the magnetic field, which is discussed as being negative (positive) for 45° (135°) [20]. In this work, we discuss only the magnitude of κ_{xy}/T.

As shown in Fig. 2(a), sample A shows the largest $|\kappa_{xy}|/T$. At 12 K, $|\kappa_{xy}|/T$ of sample A becomes larger than the half-integer quantized value $q_t/(2d)$ for $H > H_{\rm min}$. The field dependence of κ_{xy}/T of sample A becomes flat for $\mu_0 H_{\|} \sim 9$ T at lower temperatures. At the same time, the magnitude of κ_{xy}/T at the flat region becomes close to $q_t/(2d)$. On the other hand, as shown in Fig. 2(b), the magnitudes of κ_{xy}/T of samples B and C remain much smaller than $q_t/(2d)$ for all temperatures and field ranges we measured. Moreover, κ_{xy}/T of sample B shows a very different field dependence with sign changes for $H > H_{\rm min}$.

The field dependence of $|\kappa_{xy}|/T$ of sample A was further checked at lower temperatures (Fig. 3). As shown in Fig. 3, the flat field dependence of $|\kappa_{xy}|/T$ observed for 8–9 T persists down to 3.3 K at $q_t/(2d)$ within our experimental error of ±10%. These results demonstrate the reproducibility of the half-integer quantization of $|\kappa_{xy}|/T$ with respect to both magnetic field and temperature. On the other hand, compared to the data in the previous report [19], the quantization of $|\kappa_{xy}|/T$ is observed at higher fields despite the similar $H_{\rm min}$. Quantization of $|\kappa_{xy}|/T$ at higher fields was also reported in Ref. [20].

Here we discuss the sample dependence of κ_{xx} and κ_{xy}. From the previous κ_{xx} measurements for both in-plane and out-of-plane transport [25], the dominant heat carrier in α-$RuCl_3$ has been shown to be phonons. The difference in the phonon thermal conductivity of the same compound is given by the different lengths of the phonon mean free path, which is limited by scattering effects on phonons [27]. Therefore, the different magnitudes of κ_{xx} of different samples are determined by the different scattering strengths of the phonons. As shown in Fig. 1(e), all samples show a very similar field dependence with a large reduction of κ_{xx} at $H_{\rm min}$. This field dependence of κ_{xx} indicates that a magnetic-field-dependent scattering mechanism of phonons is dominant in all samples. In fact, the analysis of the temperature dependence of κ_{xx} by the Callaway model done in Ref. [25] suggested that a resonant magnetic scattering is the most dominant. Therefore, the different magnitudes of κ_{xx} in different samples are attributed to different strengths of the magnetic scatterings in phonons.

As shown in Fig. 1(f), the increase in κ_{xx} above $H_{\rm min}$ is largest in sample A and is smaller in samples B and C in

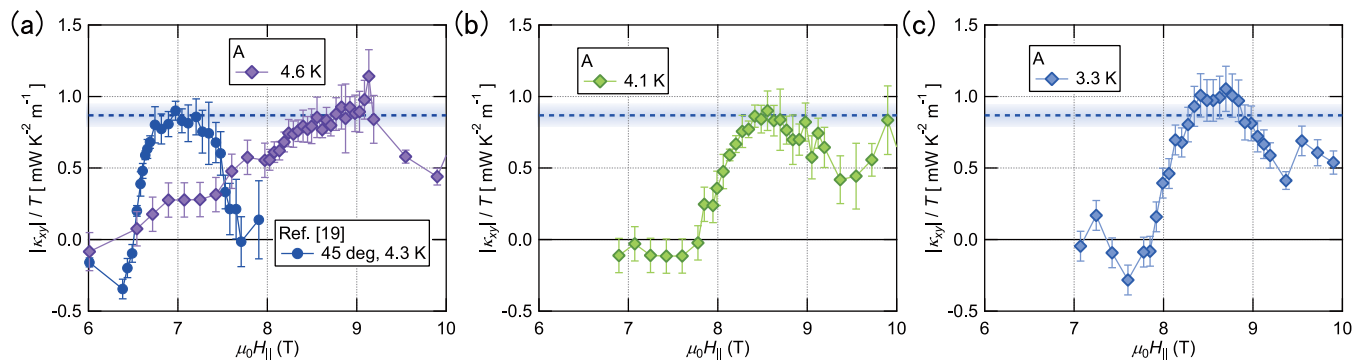

FIG. 3. The field dependence of $|\kappa_{xy}|/T$ of sample A at (a) 4.6, (b) 4.1, and (c) 3.3 K. The data in the previous report [19] are also plotted in (a). The dotted lines show the value corresponding to the half-integer quantized thermal Hall effect (see the text for details).

order of the magnitude of κ_{xx}. This sample-dependent increase above $H_{\rm min}$ shows that the magnetic-field-dependent scattering is more strongly suppressed in a sample with a larger κ_{xx}. In addition to this relation between the magnitude and the field dependence of κ_{xx}, a sample with a larger κ_{xx} shows a larger decrease of $\chi(T)$ below $T_{\rm N}$, as shown in Fig. 1(a). This decrease of $\chi(T)$ below $T_{\rm N}$ reflects the magnitude of the AFM order, showing that a larger decrease of $\chi(T)$ is observed in a sample with a better quality. Therefore, a larger field suppression of the magnetic-field-dependent scattering is observed in a better-quality sample. Given that the quantized κ_{xy} is observed only in sample A, which shows the largest suppression of the magnetic-field-dependent scattering, we conclude that the suppression of the magnetic-field-dependent scattering in a high-quality sample is necessary to realize the quantized thermal edge current. The different field region of the quantized thermal Hall in this work from that of the previous work [19] may imply that a larger magnetic field is required to stabilize the chiral edge current in our sample.

A possible mechanism for the dissipation of the quantized thermal Hall current by the magnetic scatterings of phonons is that the field-induced gap, protecting the chiral edge current, is closed by a band-broadening effect of disorders. A similar mechanism was put forward in the intrinsic AHE in ferromagnetic metals in which the intrinsic AHE was suggested to be dissipated when the energy broadening by scattering effects, which is estimated by the magnitude of the longitudinal conductivity, exceeds the energy gap formed by the spin-orbit interaction [21]. In contrast to the electric AHE, in which both longitudinal and transverse conductions are given by electrons, the thermal Hall conductivity in α-$RuCl_3$ is carried by the itinerant Majorana fermions, whereas the longitudinal thermal conductivity is carried by phonons. Thus, the scattering effects of Majorana fermions cannot be estimated from the magnitude of κ_{xx}. Meanwhile, it has been pointed out that a large coupling between the Majorana fermions and the phonons is necessary to observe the quantized thermal Hall effect [28,29]. We therefore speculate that the magnetic scattering effects of phonons, which broaden the Majorana energy bands through a spin-phonon coupling, may give rise to a closing of the Majorana gap protecting the chiral edge current. The dominant magnetic scatterings on κ_{xx} [25] and the larger field effect on κ_{xx} observed in sample A also imply that magnetic impurities, rather than nonmagnetic ones, are more relevant to the dissipation mechanism of the Majorana gap.

The effects of disorders, such as bond randomness or vacancies, on the Kitaev model have been extensively studied in theory [30–36]. Recently, it was pointed out that κ_{xx} is easily suppressed by disorders [36] and that the quantized thermal Hall effect is dissipated by a closing of the Majorana gap [36] or by the Anderson localization of the Majorana fermions [35]. These high sensitivities of κ_{xx} and κ_{xy} to disorders are consistent with our experimental results. Clarifying further details of the disorder effects on the quantized thermal Hall effect by investigating the structure of the candidate materials or by artificially introducing disorders will be an important future issue.

In summary, we have investigated the sample dependence of the thermal Hall conductivity of the Kitaev candidate material α-$RuCl_3$. We confirm the reproducibility of the half-integer quantized thermal Hall effect in the sample with the largest longitudinal thermal conductivity. We also find the magnitude of the longitudinal thermal conductivity is positively correlated with the field-induced increase of κ_{xx} and the decrease of χ below $T_{\rm N}$. We suggest that suppressing the magnetic scattering of phonons is important to realize the quantized chiral edge current.

We thank Y. Kasahara, Y. Matsuda, and T. Shibauchi for fruitful discussions. This work was supported by Grants-in-Aid for Scientific Research (KAKENHI) Grants No. 17H01142, No. 19H00648, No. 19H01848, No. 19K03711, and No. 19K21842.

[1] K. von Klitzing, The quantized Hall effect, Rev. Mod. Phys. **58**, 519 (1986).
[2] A. Kitaev, Anyons in an exactly solved model and beyond, Ann. Phys. (NY) **321**, 2 (2006).
[3] Y. Motome and J. Nasu, Hunting Majorana fermions in kitaev magnets, J. Phys. Soc. Jpn. **89**, 012002 (2020).
[4] G. Jackeli and G. Khaliullin, Mott Insulators in the Strong Spin-Orbit Coupling Limit: From Heisenberg to a Quantum Compass and Kitaev Models, Phys. Rev. Lett. **102**, 017205 (2009).
[5] K. W. Plumb, J. P. Clancy, L. J. Sandilands, V. V. Shankar, Y. F. Hu, K. S. Burch, H.-Y. Kee, and Y.-J. Kim, α-$RuCl_3$: A spin-orbit assisted Mott insulator on a honeycomb lattice, Phys. Rev. B **90**, 041112(R) (2014).
[6] H.-S. Kim, V. Shankar, V. A. Catuneanu, and H.-Y. Kee, Kitaev magnetism in honeycomb $RuCl_3$ with intermediate spin-orbit coupling, Phys. Rev. B **91**, 241110(R) (2015).
[7] S. M. Winter, A. A. Tsirlin, M. Daghofer, J. van den Brink, Y. Singh, P. Gegenwart, and R. Valentí, Models and materials for generalized Kitaev magnetism, J. Phys.: Condens. Matter **29**, 493002 (2017).
[8] S.-H. Do, S.-Y. Park, J. Yoshitake, J. Nasu, Y. Motome, Y. S. Kwon, D. T. Adroja, D. J. Voneshen, K. Kim, T.-H. Jang, J.-H. Park, K.-Y. Choi, and S. Ji, Majorana fermions in the Kitaev quantum spin system α-$RuCl_3$, Nat. Phys. **13**, 1079 (2017).
[9] L. J. Sandilands, Y. Tian, K. W. Plumb, Y.-J. Kim, and K. S. Burch, Scattering Continuum and Possible Fractionalized Excitations in α-$RuCl_3$, Phys. Rev. Lett. **114**, 147201 (2015).
[10] J. Nasu, J. Knolle, D. L. Kovrizhin, Y. Motome, and R. Moessner, Fermionic response from fractionalization in an insulating two-dimensional magnet, Nat. Phys. **12**, 912 (2016).
[11] A. Banerjee, C. A. Bridges, J.-Q. Yan, A. A. Aczel, L. Li, M. B. Stone, G. E. Granroth, M. D. Lumsden, Y. Yiu, J. Knolle, S. Bhattacharjee, D. L. Kovrizhin, R. Moessner, D. A. Tennant, D. G. Mandrus, and S. E. Nagler, Proximate Kitaev quantum spin liquid behavior in a honeycomb magnet, Nat. Mater. **15**, 733 (2016).

[12] A. Banerjee, J. Yan, J. Knolle, C. A. Bridges, M. B. Stone, M. D. Lumsden, D. G. Mandrus, D. A. Tennant, R. Moessner, and S. E. Nagler, Neutron scattering in the proximate quantum spin liquid α-$RuCl_3$, Science **356**, 1055 (2017).

[13] Y. Kasahara, K. Sugii, T. Ohnishi, M. Shimozawa, M. Yamashita, N. Kurita, H. Tanaka, J. Nasu, Y. Motome, T. Shibauchi, and Y. Matsuda, Unusual Thermal Hall Effect in a Kitaev Spin Liquid Candidate α-$RuCl_3$, Phys. Rev. Lett. **120**, 217205 (2018).

[14] Y. Kubota, H. Tanaka, T. Ono, Y. Narumi, and K. Kindo, Successive magnetic phase transitions in α-$RuCl_3$: XY-like frustrated magnet on the honeycomb lattice, Phys. Rev. B **91**, 094422 (2015).

[15] J. A. Sears, M. Songvilay, K. W. Plumb, J. P. Clancy, Y. Qiu, Y. Zhao, D. Parshall, and Y.-J. Kim, Magnetic order in α-$RuCl_3$: A honeycomb-lattice quantum magnet with strong spin-orbit coupling, Phys. Rev. B **91**, 144420 (2015).

[16] H. B. Cao, A. Banerjee, J.-Q. Yan, C. A. Bridges, M. D. Lumsden, D. G. Mandrus, D. A. Tennant, B. C. Chakoumakos, and S. E. Nagler, Low-temperature crystal and magnetic structure of α-$RuCl_3$, Phys. Rev. B **93**, 134423 (2016).

[17] R. D. Johnson, S. C. Williams, A. A. Haghighirad, J. Singleton, V. Zapf, P. Manuel, I. I. Mazin, Y. Li, H. O. Jeschke, R. Valentí, and R. Coldea, Monoclinic crystal structure of α-$RuCl_3$ and the zigzag antiferromagnetic ground state, Phys. Rev. B **92**, 235119 (2015).

[18] J. A. Sears, Y. Zhao, Z. Xu, J. W. Lynn, and Y.-J. Kim, Phase diagram of α-$RuCl_3$ in an in-plane magnetic field, Phys. Rev. B **95**, 180411(R) (2017).

[19] Y. Kasahara, T. Ohnishi, Y. Mizukami, O. Tanaka, S. Ma, K. Sugii, N. Kurita, H. Tanaka, J. Nasu, Y. Motome, T. Shibauchi, and Y. Matsuda, Majorana quantization and half-integer thermal quantum Hall effect in a Kitaev spin liquid, Nature (London) **559**, 227 (2018).

[20] T. Yokoi, S. Ma, Y. Kasahara, S. Kasahara, T. Shibauchi, N. Kurita, H. Tanaka, J. Nasu, Y. Motome, C. Hickey, S. Trebst, and Y. Matsuda, Half-integer quantized anomalous thermal Hall effect in the Kitaev material α-$RuCl_3$, arXiv:2001.01899.

[21] Y. Shiomi, Y. Onose, and Y. Tokura, Effect of scattering on intrinsic anomalous Hall effect investigated by Lorenz ratio, Phys. Rev. B **81**, 054414 (2010).

[22] M. Yamashita, M. Akazawa, M. Shimozawa, T. Shibauchi, Y. Matsuda, H. Ishikawa, T. Yajima, Z. Hiroi, M. Oda, H. Yoshida, H.-Y. Lee, J. H. Han, and N. Kawashima, Thermal-transport studies of kagomé antiferromagnets, J. Phys.: Condens. Matter **32**, 074001 (2019).

[23] P. Lampen-Kelley, S. Rachel, J. Reuther, J.-Q. Yan, A. Banerjee, C. A. Bridges, H. B. Cao, S. E. Nagler, and D. Mandrus, Anisotropic susceptibilities in the honeycomb Kitaev system α-$RuCl_3$, Phys. Rev. B **98**, 100403(R) (2018).

[24] See Supplemental Material at http://link.aps.org/supplemental/10.1103/PhysRevB.102.220404 for the temperature dependence of the heat capacity measured after the thermal-transport measurements.

[25] R. Hentrich, A. U. B. Wolter, X. Zotos, W. Brenig, D. Nowak, A. Isaeva, T. Doert, A. Banerjee, P. Lampen-Kelley, D. G. Mandrus, S. E. Nagler, J. Sears, Y.-J. Kim, B. Büchner, and C. Hess, Unusual Phonon Heat Transport in α-$RuCl_3$: Strong Spin-Phonon Scattering and Field-Induced Spin Gap, Phys. Rev. Lett. **120**, 117204 (2018).

[26] R. Hentrich, M. Roslova, A. Isaeva, T. Doert, W. Brenig, B. Büchner, and C. Hess, Large thermal Hall effect in α-$RuCl_3$: Evidence for heat transport by Kitaev-Heisenberg paramagnons, Phys. Rev. B **99**, 085136 (2019).

[27] R. Berman, *Thermal Conduction in Solids* (Clarendon, Oxford, 1976).

[28] Y. Vinkler-Aviv and A. Rosch, Approximately Quantized Thermal Hall Effect of Chiral Liquids Coupled to Phonons, Phys. Rev. X **8**, 031032 (2018).

[29] M. Ye, G. B. Halász, L. Savary, and L. Balents, Quantization of the Thermal Hall Conductivity at Small Hall Angles, Phys. Rev. Lett. **121**, 147201 (2018).

[30] A. J. Willans, J. T. Chalker, and R. Moessner, Disorder in a Quantum Spin Liquid: Flux Binding and Local Moment Formation, Phys. Rev. Lett. **104**, 237203 (2010).

[31] A. J. Willans, J. T. Chalker, and R. Moessner, Site dilution in the Kitaev honeycomb model, Phys. Rev. B **84**, 115146 (2011).

[32] V. Chua and G. A. Fiete, Exactly solvable topological chiral spin liquid with random exchange, Phys. Rev. B **84**, 195129 (2011).

[33] Santhosh G., V. Sreenath, A. Lakshminarayan, and R. Narayanan, Localized zero-energy modes in the Kitaev model with vacancy disorder, Phys. Rev. B **85**, 054204 (2012).

[34] E. C. Andrade and M. Vojta, Magnetism in spin models for depleted honeycomb-lattice iridates: Spin-glass order towards percolation, Phys. Rev. B **90**, 205112 (2014).

[35] M. G. Yamada, Anderson–Kitaev spin liquid, npj Quantum Mater. **5**, 82 (2020).

[36] J. Nasu and Y. Motome, Thermodynamic and transport properties in disordered Kitaev models, Phys. Rev. B **102**, 054437 (2020).